Development of panel loudspeaker system: Design, evaluation and enhancement

Mingsian R. Bai[a] and Talung Huang
Department of Mechanical Engineering, National Chiao-Tung University, 1001 TaHsueh Road, Hsin-Chu 300, Taiwan, Republic of China

(Received 10 July 2000; accepted for publication 13 March 2001)

Panel speakers are investigated in terms of structural vibration and acoustic radiation. A panel speaker primarily consists of a panel and an inertia exciter. Contrary to conventional speakers, flexural resonance is encouraged such that the panel vibrates as randomly as possible. Simulation tools are developed to facilitate system integration of panel speakers. In particular, electro-mechanical analogy, finite element analysis, and fast Fourier transform are employed to predict panel vibration and the acoustic radiation. Design procedures are also summarized. In order to compare the panel speakers with the conventional speakers, experimental investigations were undertaken to evaluate frequency response, directional response, sensitivity, efficiency, and harmonic distortion of both speakers. The results revealed that the panel speakers suffered from a problem of sensitivity and efficiency. To alleviate the problem, a woofer using electronic compensation based on H_2 model matching principle is utilized to supplement the bass response. As indicated in the result, significant improvement over the panel speaker alone was achieved by using the combined panel-woofer system.
[DOI: 10.1121/1.1371544]

PACS numbers: 43.38.Ja, 43.38.Ar [SLE]

I. INTRODUCTION

For decades, the design concept of conventional loudspeaker has been centered at the principle of rigid piston. The common practice is to make the diaphragm of the loudspeaker as light and stiff as possible such that the loudspeaker behaves as a rigid piston. Furthermore, the surface is generally made conical to further increase rigidity as well as on-axis sensitivity at low frequency. Although the technology is well established, conventional loudspeakers suffer from a problem: the sound generated by conventional loudspeakers becomes increasingly directional for high frequencies. This ''beaming'' effect results in the drop of sound power at the high frequency region. Consequently an audio system generally requires crossover circuits and multi-way loudspeakers to cover the audible frequency range, which makes the entire system unnecessarily large.

Panel speakers are based on a philosophy contradicting conventional design (Azima, 1998). A panel loudspeaker primarily consists of a panel and an inertia exciter (Fig. 1). The exciter is essentially a voice-coil driver with the coil attached to the panel. The magnet serves as a proof mass to produce inertia force. In lieu of a rigid diaphragm as used in conventional loudspeakers, flexible panels are employed as the primary sound radiators. Resonance of flexural motion is encouraged such that the panel vibrates as randomly as possible. The sound field produced by this type of *distributed mode loudspeaker* (DML) is very diffuse at high frequency. As claimed by the supporters of panel speakers, DML provide advantages over the conventional counterpart such as compactness, linear on-axis, attenuation, insensitivity to room conditions, bi-polar radiation, good linearity, and so forth (Azima, 1998). Of particular interest is that the DML has a less pronounced beaming problem at high frequencies than conventional loudspeakers, which bypass the need for crossover circuits and multi-way high frequency speakers. DML began to find applications in multimedia, notebook computers, mobile phones, high-fidelity audio systems, public addressing systems, projection screens, pictures, and decorations (Azima, 1998).

Although commercial panel speakers may have been around for more than a decade, only recently has this concept been subjected to scientific analysis devoted to electroacoustics design. In this paper, the operating principles of DML are investigated in terms of structural vibration and acoustic radiation. Simulation tools are developed prior to integration of a DML system. Specifically, electro-mechanical analogy is employed for modeling the panel-exciter system. Finite element analysis is used in the determination of aspect ratios of the panel and calculation of panel vibration. Two-dimensional fast Fourier transform (FFT) is utilized to predict the acoustic radiation. In order to compare DML with conventional loudspeakers, experiments were undertaken to evaluate frequency response, directional response, sensitivity, efficiency, and harmonic distortion of both speakers.

It was found in the comparison that the DML produced desirable omni-directional response, even at high frequency. Nevertheless, the DML suffered from the problem of poor sensitivity and efficiency. This price that DML have to pay is mainly due to the *hydrodynamic short circuit* of flexible panels vibrating below coincidence (Cremer and Heckl, 1988). To overcome the physical constraint, a woofer using electronic compensation based on the H_2 model matching principle is used to supplement the bass response. Electronic

[a]Electronic mail: msbai@cc.nctu.edu.tw

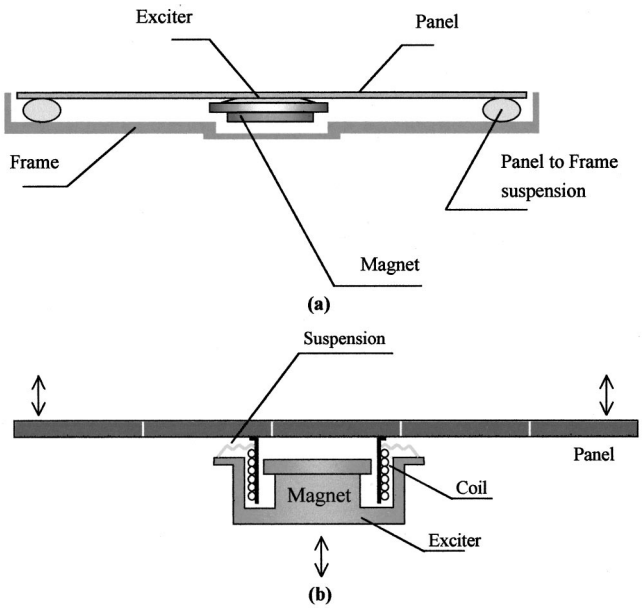

FIG. 1. Schematic of a DML. (a) The panel loudspeaker consisting of a panel and an exciter; (b) details of the intertia exciter.

compensation was realized by a digital signal processor (DSP). Experimental investigation showed that significant improvement of the combined system over the panel loudspeaker was achieved.

II. RATIONALES OF PANEL LOUDSPEAKERS

The operating principle of DML is based on acoustic radiation of modal bending waves. In contrast to conventional loudspeaker design, resonance of flexural motion is encouraged such that the panel will vibrate as randomly as possible. When excited, the flexible panel of a DML develops complex and dense vibration modes uniformly distributed over its entire surface and operating frequency range. The beaming effect of DML is generally not as pronounced as the coherent field of a rigid piston because the sound field radiated by a DML is very diffuse at high frequency. The panel of a DML can be modeled as a thin plate described by

$$d\nabla^4 w+\mu\frac{\partial^2 w}{\partial t^2}=0, \tag{1}$$

where w is the normal displacement, μ is mass per unit surface area,

$$\nabla^4=\left(\frac{\partial^2}{\partial x^2}+\frac{\partial^2}{\partial y^2}\right)^2$$

is the bi-harmonic operator, and

$$D=\frac{Eh^3}{12(1-\nu^2)} \tag{2}$$

is the bending stiffness per unit width of the plate (E, ν, and h are Young's modulus, Poisson ratio, and thickness, respectively). If there exists only a time-harmonic bending wave traveling in x-direction, Eq. (1) admits the general solution

$$w(x,t)=(C_1E^{-jk_bx}+C_2e^{jk_bx}+C_3e^{-k_bx}+C_4e^{k_bx})e^{j\omega t}, \tag{3}$$

where

$$k_b=\sqrt[4]{\omega^2\mu/D} \tag{4}$$

is called the free bending wave number, ω is angular frequency, and C_1, C_2, C_3, and C_4 are constants to be determined by boundary conditions. Note that the first two terms in Eq. (3) correspond to traveling components and the last two terms are evanescent components.

On the other hand, the sound pressure generated by the vibrating panel satisfies the linear wave equation

$$\nabla^2 p-\frac{1}{c^2}\frac{\partial^2 p}{\partial t^2}=0, \tag{5}$$

where p is sound pressure and c is sound speed. For time-harmonic field, this reduces to the Helmholtz equation

$$\nabla^2 p+k^2 p=0, \tag{6}$$

where $k=\omega/c$ is the wave number of sound wave.

The fundamental difference between a DML and a conventional loudspeaker lies in that the mechanical impedance of a point-excited infinite panel is a frequency-independent real constant (Morse and Ingard, 1986):

$$z_m=8\sqrt{D\mu}. \tag{7}$$

This property enables us to derive a constant driving-point velocity ν_c from a constant force f_e, which is approximately true for an electro-magnetic exciter driven by a constant current. In addition, it can be shown that the sound power W_R of a randomly vibrating panel is proportional to the time and space averaged square velocity $\langle\overline{\nu^2}\rangle$ which is also proportional to the driving-point velocity ν_c (Morse and Ingard, 1986). As a consequence, the panel would radiate constant sound power when driven by a constant force, i.e., $W_R \approx$ constant.

However, this is not the case for a conventional moving-coil loudspeaker. At the mass-controlled region, its cone acceleration is nearly constant with respect to frequency, i.e., the cone velocity is inversely proportional to frequency ($\nu_c \sim \omega^{-1}$). In the high frequency range ($ka \gg 1$), the radiation resistance R_R of a rigid piston is nearly constant (Beranek, 1996). Thus the sound power radiated by a conventional loudspeaker has the frequency dependence as

$$W_R=\tfrac{1}{2}R_R|\nu_c|^2\sim\omega^0\omega^{-2}=\omega^{-2}. \tag{8}$$

The radiation power drops as frequency increases (-20 dB/decade), even though the on-axis sound pressure remains constant. The main contributing factor to this power drop is the beaming effect resulting from the coherent phase motion of a rigid piston. In the case of a DML, the beaming effect would not be as pronounced because the sound field generated by the random panel vibration is ''quasi-diffuse.''

On the basis of panel velocity, the radiated sound pressure from the planar source can be calculated using the Rayleigh's integral (Kinsler *et al.*, 1982):

$$p(x,y,z)=-jk\rho_0 c\int_{-\infty}^{\infty}\int_{-\infty}^{\infty}\frac{e^{jkR}}{R}\nu(x_0,y_0)dx_0\,dy_0, \tag{9}$$

where ρ_0 is the density of air, (x,y,z) and $(x_0,y_0,0)$ are the field point and the source point, respectively, and R

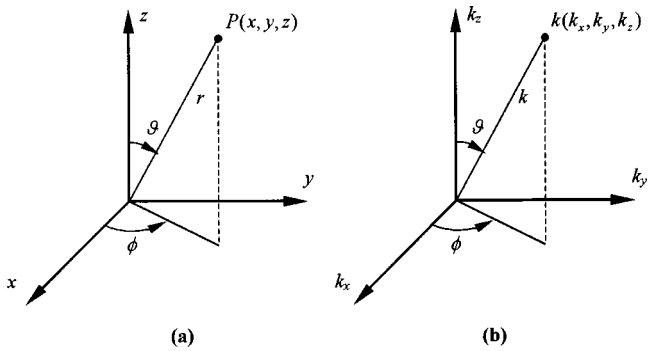

FIG. 2. Coordinate system for sound radiation analysis. (a) Spatial domain; (b) wave number domain.

$=\sqrt{(x-x_0)^2+(y-y_0)^2+(z-z_0)^2}$. In the far field, this integral can be rewritten as (Morse and Ingard, 1986)

$$p(x,y,z)\approx -jk\rho_0 c\frac{e^{jkr}}{r}V(k_x,k_y), \tag{10}$$

where $k_x=k\sin\vartheta\cos\phi$, $k_y=k\sin\vartheta\sin\phi$, $k_z=k\cos\vartheta$, $r=\sqrt{x^2+y^2+z^2}$, r, ϑ, and ϕ are spherical coordinates (Fig. 2), and $V(k_x,k_y)$ is the spatial Fourier transform of $\nu(x,y)$:

$$V(k_x,k_y)\equiv\int_{-\infty}^{\infty}\int_{-\infty}^{\infty}\nu(x,y)e^{-j(k_x x+k_y y)}\,dx\,dy. \tag{11}$$

Equation (10) implies that the far-field directivity of the source depends on the velocity spectrum on the wave number space. Only the propagating modes inside the radiation circle ($k_x^2+k_y^2\leqslant k^2$) contribute to the far-field radiation.

Classical theory of plate radiation has suggested a *hydrodynamic short circuit* phenomenon: a flexible infinite panel has no acoustic output at frequencies below the *coincidence frequency* (Cremer and Heckl, 1988)

$$\omega_c=c^2\sqrt{\frac{\mu}{D}} \tag{12}$$

at which the speed of sound matches the speed of bending wave in a panel. However, this is not true for a ''finite'' panel and it is possible to have sound radiation below coincidence due to the aperture effect. A finite panel can be described by an aperture function

$$a(x,y)=\begin{cases}1, & (x,y)\text{ inside aperture}\\ 0, & (x,y)\text{ outside aperture}\end{cases}. \tag{13}$$

By decomposing the flexural standing waves into traveling waves, the velocity distribution of the finite panel $\nu'(x,y)$ can be approximated in terms of the velocity distribution of an infinite panel $\nu(x,y)$,

$$\nu'(x,y)=\nu(x,y)a(x,y). \tag{14}$$

In wave number space, this amounts to

$$V'(k_x,k_y)=V(k_x,k_y)*A(k_x,k_y), \tag{15}$$

where ''*'' denotes convolution. Hence the aperture effect results in leakage of the wave number spectrum such that the panel could have nonzero acoustic output into the far field below coincidence (Panzer and Harris, 1998a). For example, a one-dimensional surface velocity distribution $\nu(x)=\cos(k_b x)$ (expressed as a standing wave due to boundary effects) corresponds to the velocity spectra in wave number space and the radiation patterns shown in Fig. 3. Even though ideal hydrodynamic short circuit no longer exists in such case, the acoustic radiation at low frequency remains not as efficient as rigid pistons because of cancellations of volume velocity on the surface. In addition, it was pointed out by the reviewer that the presence of boundaries will cause only evanescent waves. The boundary effects are not considered in the above arguments in that the differences in the subsonic portion of the wave number spectra of the finite and infinite plate responses have no effect on the far-field radiation (Junger and Feit, 1986).

III. SYSTEM MODELING AND SIMULATION

Simulation tools were developed to facilitate the design and integration of DML. These tools encompass two aspects: electro-mechanical modeling and acoustic radiation prediction.

A. Electro-mechanical modeling

Electro-mechanical equivalent circuit technique is employed for modeling the panel-exciter system of a DML. The equivalent circuit (mobility analogy) of a DML system is shown in Fig. 4(a). Although the equivalent circuit in Fig. 4(a) is in the form of graphic language, it is entirely based on Newton's second law, Lorentz force, and Kirchhoff's circuit laws. The details of how this circuit is derived are tedious but standard in literature, e.g., text by Beranek (1996) and are thus omitted for brevity. In this figure, $Z_c=R_c+jX_c$ is the electrical impedance of voice coil. Bl is the motor constant of the voice coil. C_s and R_s are the compliance and damping, respectively, between the magnet and the panel. M_m is the mass of the magnet assembly. M_c is the mass of the voice coil. Z_m is the mechanical impedance of an infinite panel at the driving point. M_f is the mass of the frame. C_p and R_p are the compliance and damping of the suspension between the panel and frame. Note that the constant real driving point impedance of Eq. (7) for an infinite plate is used and radiation loading is neglected in the modeling. It has been pointed out by the reviewer that the force on the plate should be dependent on the impedance predicted by the finite element model. The ''coupled'' electrical-mechanical-acoustical systems should be solved simultaneously. For the present, this is somewhat impractical from the engineering standpoint. In this work, we are merely content with the frequency-independent impedance of an infinite plate. This is a reasonable simplification because only far-field radiation is of interest (so that evanescent waves due to boundary effects are negligible) and also the panel is much heavier than the diaphragms of cone speakers (so that acoustic loading is negligible).

The equivalent circuit can be simplified into a Thevenin circuit of Fig. 4(b), where V_s is the voltage source, Z_s is the source impedance reflected to the mechanical side, and Z_L is the mechanical impedance of the load including the panel and the exciter assembly. The force is determined with the attached driver assembly taken into account. In terms of the Laplace transform,

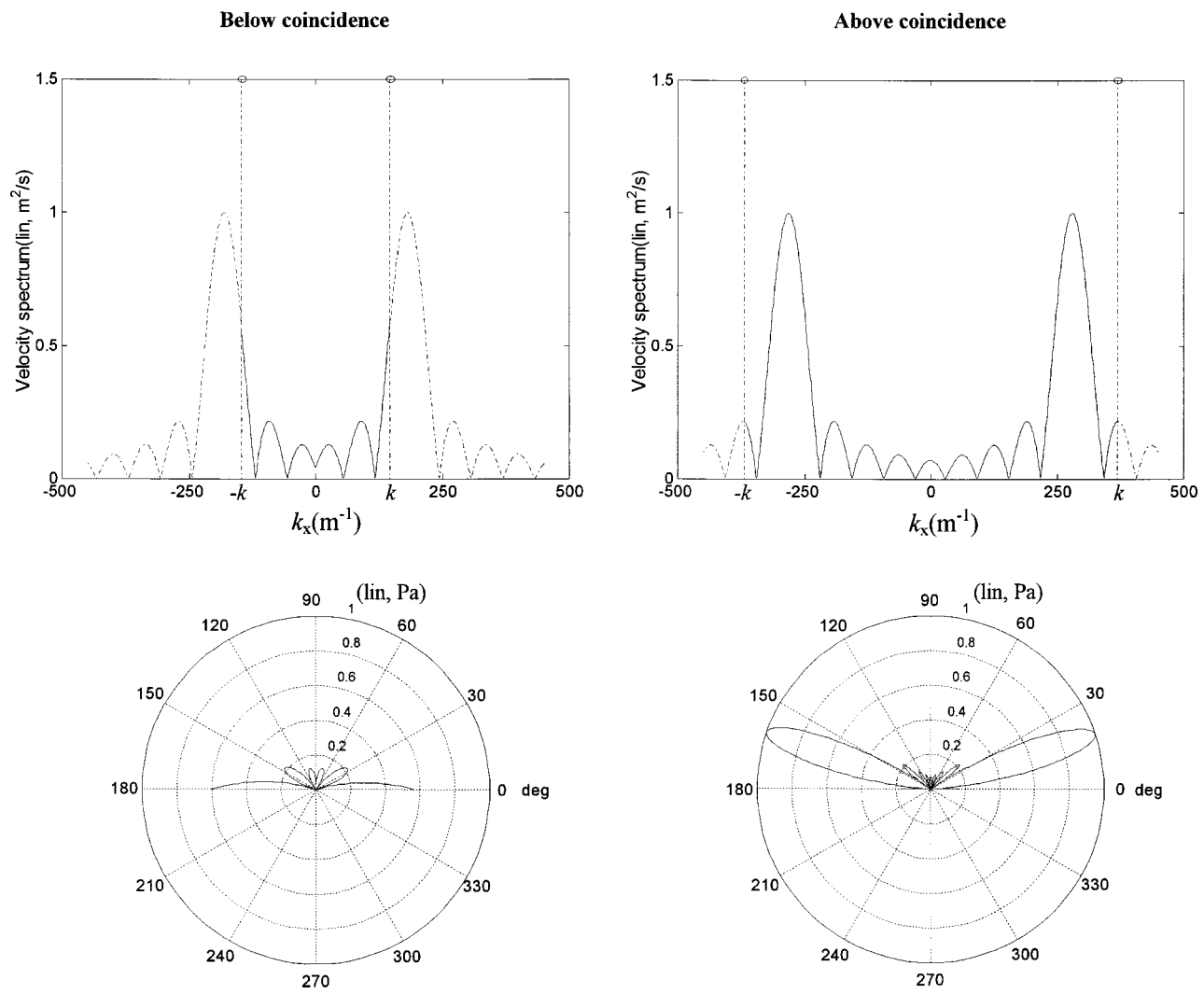

FIG. 3. Sound radiation of a vibrating panel with an aperture 0.2 m. The figures in the upper part are the velocity spectra in wave number domain, while the figures in the lower part are the polar radiation patterns. (a) Below coincidence ($f=8$ kHz, $k_b=180\ \mathrm{m}^{-1}$, $k=148\ \mathrm{m}^{-1}$); (b) above coincidence ($f=18$ kHz, $k_b=294\ \mathrm{m}^{-1}$, $k=368\ \mathrm{m}^{-1}$).

$$V_s(s)=\frac{N_1(s)}{D_1(s)}, \tag{16}$$

where

$$N_1(s)=Bl\cdot C_s\cdot Eg\cdot M_m s$$

and

$$\begin{aligned} D_1(s)=&C_sM_mM_cX_cs^3+(C_sM_mM_cR_c+C_sM_mR_sX_c\\ &+C_sM_cR_sX_c)s^2+(Bl^2C_sM_c+Bl^2C_sM_m\\ &+C_sM_mR_sR_c+C_sM_cR_sR_c+M_mX_c+M_cX_c)s\\ &+(M_m+M_c)R_c, \end{aligned} \tag{17}$$

$$Z_s(s)=\frac{N_2(s)}{D_2(s)},$$

where

$$\begin{aligned} N_2(s)=&C_sM_mX_cs^3+(C_sM_mR_c+X_c+C_sR_sX_c)s^2\\ &+(Bl^2C_s+C_sR_sR_c)s+R_c \end{aligned}$$

and

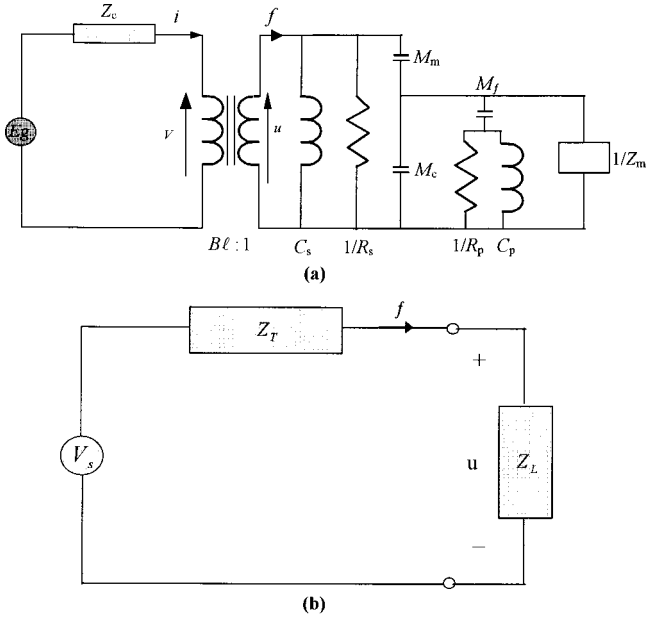

FIG. 4. Electro-mechanical analogy of a DML. (a) Equivalent circuit (mobility analogy); (b) simplified circuit. The symbols f and u in the figures denote, respectively, the force and the velocity of the panel.

TABLE I. Parameters of the panel and the exciter.

	Parameters
Panel	Bending stiffness $D=1.672\ \mathrm{N\cdot m}$
	Area density $\mu=0.492\ \mathrm{kg/m^2}$
	Dimension $=0.2\ \mathrm{m}\times 0.112\ \mathrm{m}\times 0.002\ \mathrm{m}$
	Poisson ratio $\nu=0.33$
	Mass of frame $M_f=0.06\ \mathrm{kg}$
	Panel mobility $Z_{mp}=7.255\ \mathrm{N\cdot s/m}$
	Damping of panel suspension $R_p=0\ \mathrm{N\cdot s/m}$
	Compliance of panel suspension $C_p=900\times 10^{-6}\ \mathrm{m/N}$
Exciter	Impedance of voice coil $Z_c=4+j\omega\cdot 32\times 10^{-6}\ \Omega$
	Motor constant $Bl=1.54\ \mathrm{Wb/m}$
	Compliance of coil suspension $C_s=170\times 10^{-6}\ \mathrm{m/N}$
	Damping of panel suspension $R_s=0.257\ \mathrm{N\cdot s/m}$
	Mass of magnet $M_m=37\times 10^{-3}\ \mathrm{kg}$
	Mass of coil $M_c=0.35\times 10^{-3}\ \mathrm{kg}$

$$
\begin{aligned}
D_2(s)=s[&C_sM_cM_mX_cs^3+(C_sM_mM_cR_c+C_sM_mR_sX_c\\
&+C_sM_cR_sX_c)s^2+(Bl^2C_sM_m+Bl^2C_sM_c\\
&+C_sM_mR_sR_c+C_sM_cR_sR_c+M_mX_c+M_cX_c)s\\
&+(M_m+M_c)R_c,\\
Z_L(s)=&\frac{1}{Z_{mp}(s)}.
\end{aligned}
\tag{18}
$$

Thus the power delivered to the load $Z_L(=R_L+jX_L)$ can be calculated as

$$
W_L=\frac{|V_s|^2R_L}{(R_s+R_L)^2+(X_s+X_L)^2}. \tag{19}
$$

In the work, a DML intended for multi-media application is examined. The parameters of the panel and exciter are listed in Table I. The simulation result of the exciter force f with a sinusoidal input of 1 V rms is shown in Fig. 5.

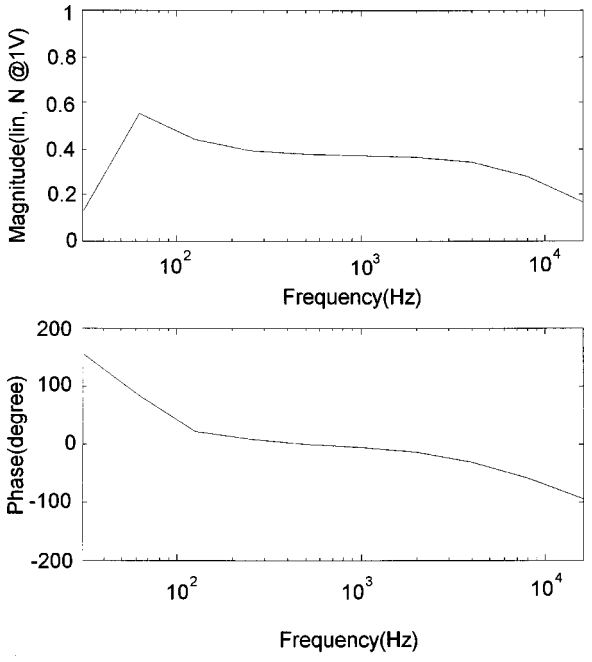

FIG. 5. Predicted force response of the exciter with 1 V rms electrical input.

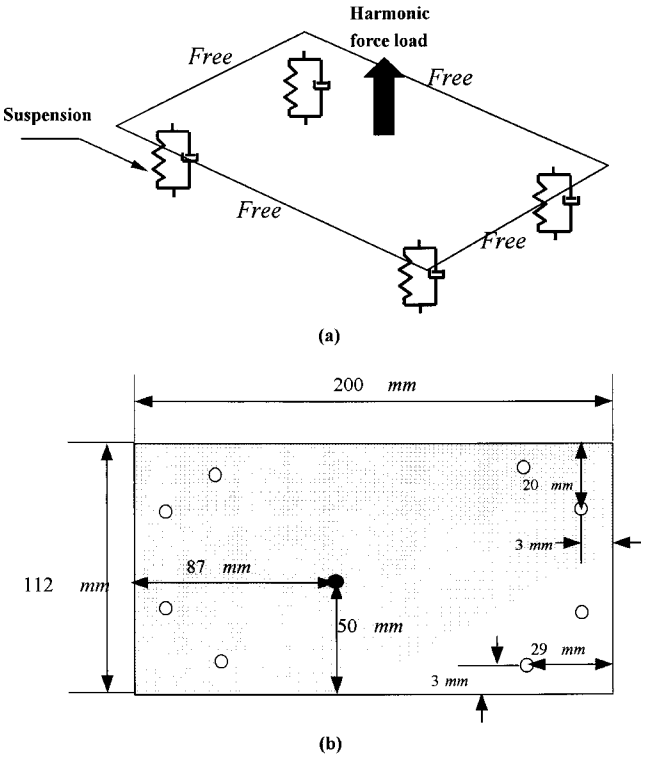

FIG. 6. Panel configuration for finite element analysis. (a) Panel driven by a harmonic concentrated force input. The panel is flexibly suspended with free boundaries; (b) dimensions of the panel and locations of the driving point (solid) and the suspensions (hollow).

B. Prediction of acoustic radiation

After the exciter force output f is determined, the surface velocity of the panel is calculated by the finite element method. A 200 mm$\times$112 mm rectangular polyurethane (PU) foam panel is examined. The locations of exciter and suspensions are shown in Fig. 6. From the finite element analysis, a sample surface velocity $v'(x,y)$ of the panel is shown in Fig. 7(a).

Having obtained surface velocity, one shall proceed with the calculation of far-field sound pressure $p(x,y,z)$ through the use of Eq. (10). In this step, two-dimensional FFT is employed to obtain the surface velocity spectrum $V'(k_x,k_y)$ in the wave number domain [Fig. 7(b)]. In this step, zero-padding (indicated in the figure) is used to improve resolution in the wave number space. The frequency response of the vibrating panel between the force input and sound pressure output at 1 m distance is calculated (Fig. 8). Combining the frequency response functions in Figs. 5 and 8 leads to the overall frequency response from the voltage input to the sound pressure output at 1 m distance (Fig. 9). In addition, directional response can also be calculated (Fig. 10). In some cases, the rms pressure within a band is required. This can be done by a straightforward integration:

$$
p_{\mathrm{rms}}=\left(\int_{f_1}^{f_2}|p(f)|^2\cdot G_{xx}\,df\right)^{1/2}, \tag{20}
$$

where f_1 and f_2 are the lower and the upper frequency limits, respectively, $p(f)$ is the frequency response between the voltage input and the sound pressure output, and G_{xx} is the power spectrum density of the input voltage.

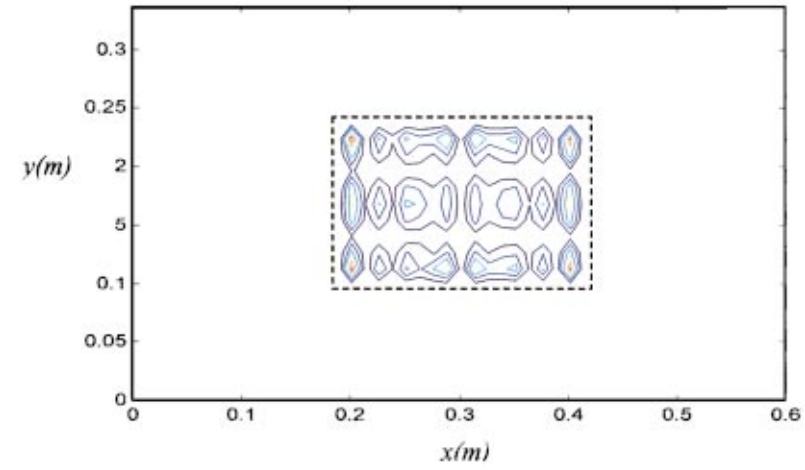

(a)

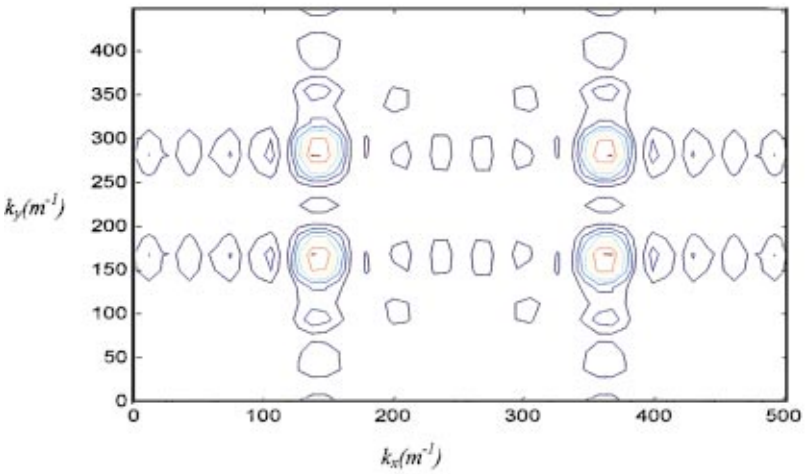

(b)

FIG. 7. Surface velocity of the panel excited by a 1 N harmonic (4 kHz) concentrated force. (a) Spatial domain; (b) wave number domain. Interior of the marked rectangle is the panel area; exterior of the marked rectangle is padded with zeros for improving resolution in the wave number space.

On the other hand, if sound power is of interest, the following formula can be utilized to calculate the power frequency response (Cremer and Heckl, 1988):

$$W(f)=\frac{\rho_0 ck}{8\pi^2}\int_{-k}^{k}\int_{-k}^{k}\frac{|V'(k_x,k_y)|^2}{\sqrt{k^2-k_x^2-k_y^2}}dk_x\,dk_y, \tag{21}$$

which entails again the surface velocity spectrum. A sample result of sound power is shown in Fig. 11. The total power within a band can be obtained from the following integration:

$$W_{\text{total}}=\int_{f_1}^{f_2}W(f)\cdot G_{xx}\,df. \tag{22}$$

IV. DESIGN PROCEDURE AND PERFORMANCE EVALUATION

A. Design procedures

The design procedures of DML are outlined as follows:

(1) Choose the area A of panel according to the specific application. In theory, a large area is preferable if efficiency is the major concern. In practice, however, the choice relies largely on packaging or artistic consideration for the application of interest. In our case, $A=0.0224\,\text{m}^2$, which is typical for multimedia or notebook applications.

(2) Choose D/μ ratio to achieve the fundamental frequency f_0 that is sufficiently low to produce reasonable low frequency response. The fundamental frequency of an isotropic vibrating plate can be approximated by (Leissa, 1993)

$$f_0\approx\frac{\pi}{A}\sqrt{\frac{D}{\mu}}. \tag{23}$$

In our case, $D/\mu=3.3984\,\text{N}\cdot\text{m}^3/\text{kg}$, $f_0=258\,\text{Hz}$, $\omega_c=64\,177\,\text{rad/s}$. Small D, or small μ, should be selected for a small panel.

(3) Minimize the panel mechanical impedance Z_m to achieve acceptable efficiency by choosing appropriate density ρ and Young's modulus E. Note that

$$Z_m=8\sqrt{D\mu}=16\frac{D}{\mu}\sqrt{3(1-\nu^2)\frac{\rho^3}{E}}. \tag{24}$$

For good acoustical efficiency, the chosen panel should be stiff (large E) and light (small ρ), e.g., composite and

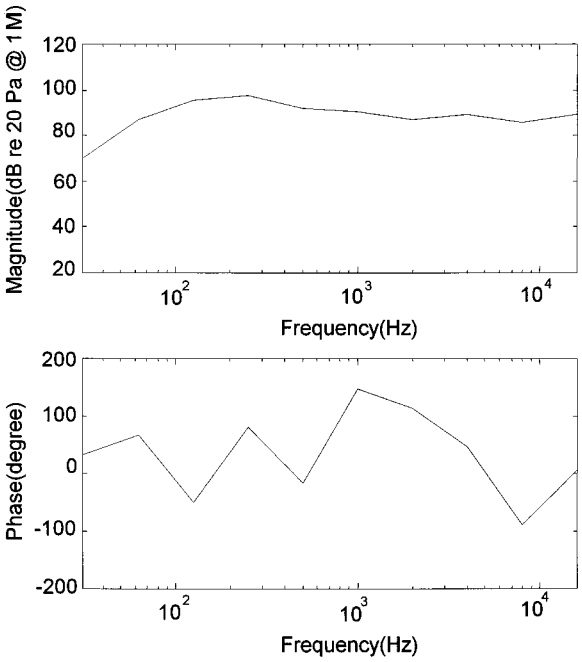

FIG. 8. Predicted frequency response of the vibrating panel between the force input and sound pressure output at 1 m on-axis distance.

honeycomb materials. Note that ρ is more critical than E in that Z_m is inversely proportional to $\sqrt{E/\rho^3}$.

(4) Choose the aspect ratio of the panel. As mentioned previously, flexural resonance is encouraged to excite as many as possible complex vibration modes in a panel. To this end, the vibration modes of panel are approximated by the product of two sets of ''beam'' modes along each side of the panel (Harris and Hawksford, 1997). For an Euler beam of length l, material constants D, μ, free at both ends, the resonance frequencies are

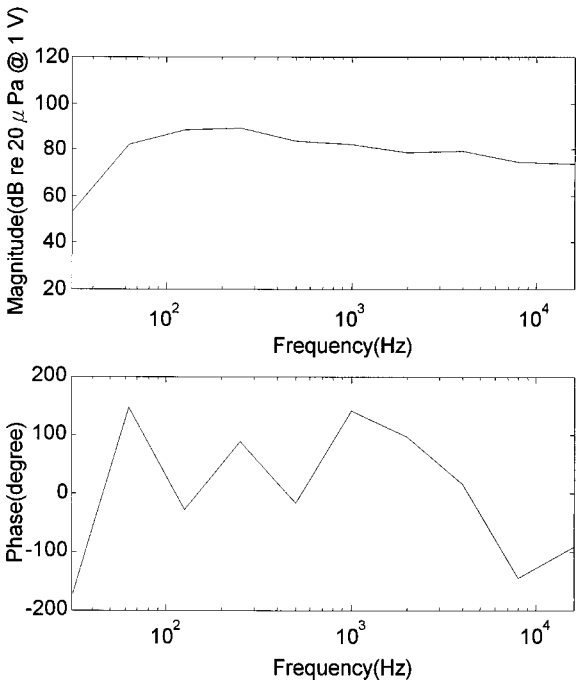

FIG. 9. Predicted overall frequency response of the DML between the voltage input and sound pressure output at 1 m on-axis distance.

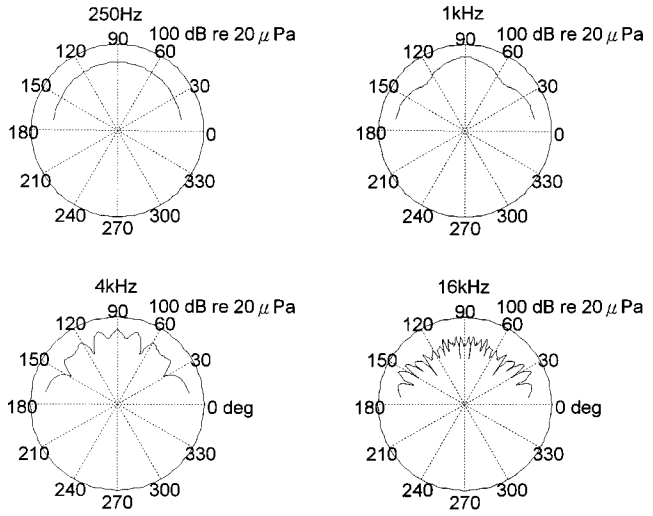

FIG. 10. Predicted directional response of the DML at 250, 1000, 4000, and 16 000 kHz for 1 W input.

$$\omega_i = \sqrt{\frac{\lambda_1^4 D}{\mu}}, \quad i = 1,2,3\cdots, \tag{25}$$

with

$$\lambda_i = \left(\frac{(2i-1)\pi}{2l}\right), \quad 1,2,3\cdots.$$

Complex vibration modes of a DML can be achieved by selecting an aspect ratio such that the beam modes along each side are best interleaved.

(5) Choose the driving point and suspension points of the panel. This can be done by a finite element based modal analysis. The driving point should be chosen at where the least nodal lines are, while the suspension points should be chosen at where the most nodal lines cross.

(6) Choose an exciter that matches the panel. A common practice is to choose a large Bl constant for ensuring sufficient output level. This is preferably achieved by using strong magnet rather than increasing the length of coil because the latter approach has an adverse effect of increasing resistance and inductance. Next, choose a

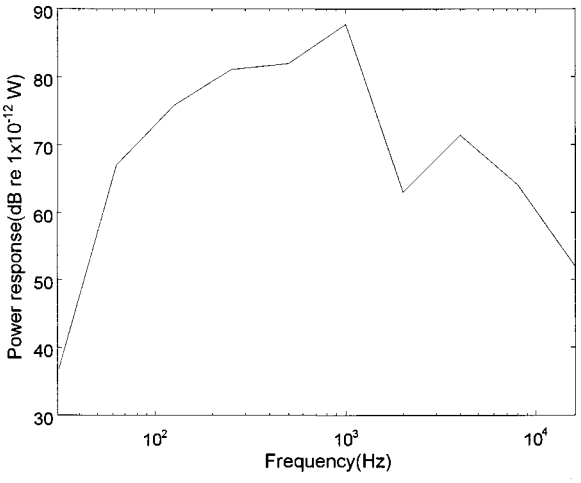

FIG. 11. Predicted sound power frequency response of the DML for 1 V rms electrical input.

large magnet mass M_m and a small coil mass M_c because the bandwidth is dependent of the ratio M_m/M_c (Panzer and Harris, 1998b).

(7) Calculate the response by the aforementioned simulation procedures. From the simulation, one can get an idea of the performance of a DML before it is practically implemented.

B. Performance evaluation

To compare the DML with the conventional loudspeaker, experimental investigations were undertaken. A conventional multimedia loudspeaker (4Ω, 2 W, 6 cm diameter) for a desktop computer was used in the comparison. The area ratio between the DML and the conventional speaker is approximately 8 to 1. Both speakers are embedded in a 1.5 m×2.0 m baffle. The enclosure of the multimedia speaker has been removed. The use of baffle is to meet the requirement of far-field calculation using Fourier transform, where rigid baffled planar sources are assumed. The performance indices to be measured are summarized as follows (Borwick, 1994).

1. Frequency response

The on-axis pressure responses at 1 m·W condition from the conventional speaker and the DML were measured in a semi-anechoic room such that the effect of room response can be minimized. Random noise band-limited to 16 kHz was used as the input. From the result of sound pressure spectral levels (Fig. 12), a significant gap (maximum 15 dB *re*: 20 μPa at 1 m·W) can be seen between the response levels.

2. Directional response

The microphone is positioned along a semi-circle at angles from 0° to 180° with 10° increments. Figure 13 shows the measured directional response of the DML versus the conventional speaker. Only data in half space are shown because both speakers are embedded in the baffle. The result indicates that DML yields an omni-directional response, even at high frequency (16 kHz). The conventional speaker does not show the kind of high frequency beaming because it is very small. If a larger DML were compared with a larger cone speaker, the contrast would be more apparent.

3. Sensitivity

The sensitivity of a speaker is defined as the free-field sound pressure level produced by 1 W electrical input, measured at the on-axis distance 1 m. In our case, a random noise input of 2 V rms (band-limited to 16 kHz) and nominal impedance of 4Ω in the coil was used. The measured sensitivities of the DML and the conventional speaker are 80.7 dB and 90.6 dB, respectively, *re*: 20 μPa over a 16 kHz band.

4. Efficiency

The efficiency of a speaker is defined as the ratio of the radiated acoustic power to the electrical power input. In the work, ISO 3745 was employed for measuring the sound power in the semi-anechoic room (ISO standard, 1977). The measured efficiencies of the DML and the conventional speaker are 0.039% and 0.089%, respectively. The result indicates the DML has a problem of sensitivity and efficiency in comparison with the conventional speaker. Poor radiation efficiency below coincidence frequency is a physical constraint of flexible panels.

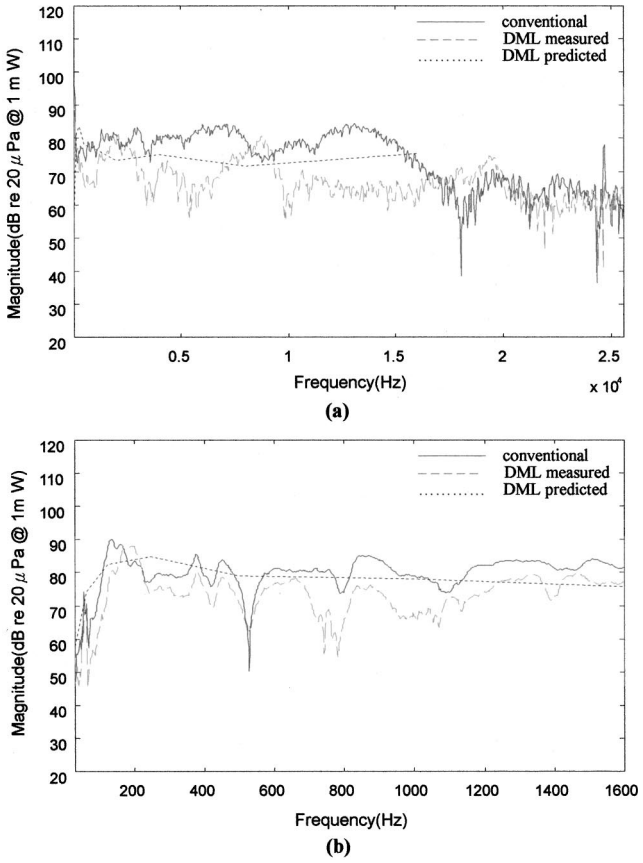

FIG. 12. The sound pressure spectral levels of the conventional speaker and the DML. The measurements are under 1 m·W condition. (a) Bandwidth = 25.6 kHz; (b) bandwidth = 1.6 kHz.

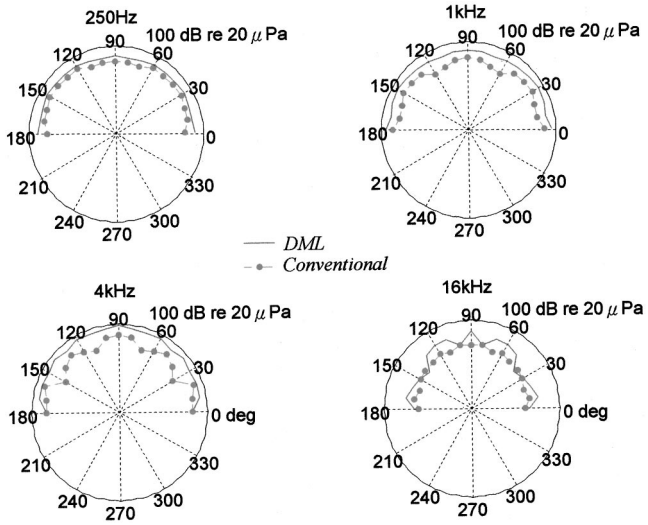

FIG. 13. Directional responses of the DML and the conventional speaker at 250, 1000, 4000, and 16 000 kHz, respectively. The radial scales are in dB with a full scale 100 dB *re*: 20 μPa.

TABLE II. Harmonic distortion of panel loudspeaker in comparison with conventional loudspeaker.

	250 Hz	1 kHz	4 kHz
Conventional speaker	1.96%	0.91%	1.02%
Panel speaker	3.25%	10.6%	12.6%

5. Harmonic distortion

Harmonic distortion represents the ratio of the rms distortion to the rms total signal. It can be calculated by measuring the rms total signal, using the same setup as for frequency response measurements and also that obtained when the driving frequency is filtered out. The harmonic distortions of the DML and the conventional loudspeaker measured with a 2 V rms and 1 W electrical input at three frequencies are summarized in Table II. The DML appears to have higher harmonic distortion than the conventional speaker does. A possible explanation is that the DML relies on resonant modes of the panel, where nonlinearity may arise due to an exceedingly large amplitude of motion at resonance.

V. SYSTEM ENHANCEMENT

The foregoing comparison between the DML and the conventional speaker reveals that the DML suffers from the problem of poor sensitivity and efficiency. In this work, a practical solution is adopted in an attempt to alleviate the problem. Such approach involves the use of an electronically compensated woofer to supplement the low frequency response.

The system consists of a woofer cascaded with a feedforward controller. The complete DML-woofer system is shown in Fig. 14(a). The design of the controller is based on a H_2 model matching idea. The system block diagram is shown in Fig. 14(b), where T_1 is the desired response model,

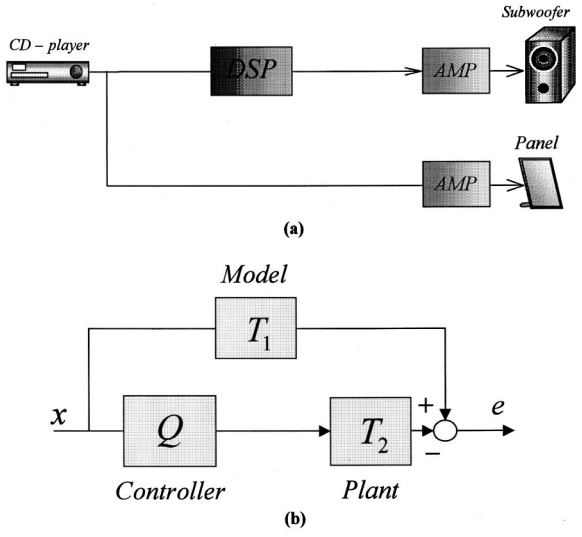

FIG. 14. The DML system enhanced by electronic compensation. (a) Integrated system of the DML and a woofer; (b) block diagram of the H_2 model matching method.

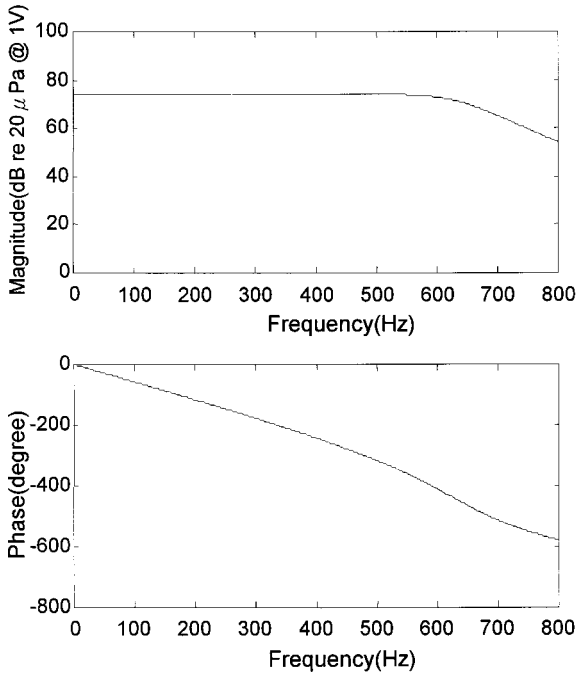

FIG. 15. Frequency response function of the desired model.

the plant T_2 is the woofer, and Q is the feedforward controller. In general, a low-pass filter with linear phase characteristics is selected as the model T_1, which is essentially similar to the low frequency crossover in conventional woofer design. The design problem is to find a proper and stable (denoted as RH^∞) transfer function Q such that the following cost function is minimized

$$J = \min_{Q \in RH^\infty} \|T_1 - T_2\|_2^2, \tag{26}$$

where ''$\|\ \|_2$'' denotes the 2-norm defined as

$$\|G(z)\|_2 \triangleq \left(\frac{1}{2\pi} \int_{-\pi}^{\pi} |G(e^{j\theta})|^2 \, d\theta \right)^{1/2}, \tag{27}$$

where z and θ are z-transform variable and digital frequency, respectively. It can be shown that the optimal solution of this problem is (Doyle *et al.*, 1992)

$$Q = T_{2m}^{-1} (T_{2a}^{-1} T_1)_s, \tag{28}$$

where T_{2m} is the minimum phase part of T_2, T_{a2} is an all pass function and the subscript s denotes the ''stable part.''

In the paper, a ninth-order low-pass filter with cutoff frequency 600 Hz is chosen as the model T_1 (Fig. 15). The frequency response of the plant is shown in Fig. 16. The plant model was found by MATLAB command *invfreqz* (Grace and Laub, 1992) and regenerated in the same plot. By using H_2 modal matching, the optimal controller is calculated, as shown in the frequency response of Fig. 17. The controller was then implemented on the platform of a floating-point DSP, TMS320C31, with a sampling rate of 2 kHz. Figure 18 compares the sound pressure frequency responses of the DML alone, the DML with woofer, and the DML with bass-enhanced woofer. The experimental result demonstrated the significant improvement of overall performance by using the woofer and electronic compensation.

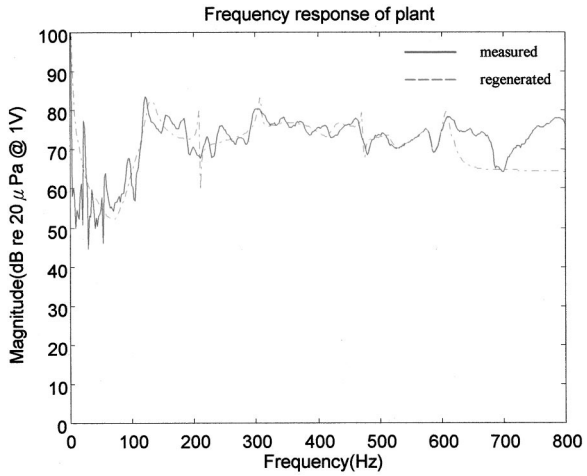

FIG. 16. Frequency response function of the plant. Solid line denotes the measured response and dash line the response regenerated from the curve fit model.

VI. CONCLUSIONS

In the paper, panel speakers were analyzed in terms of structural vibration and acoustic radiation. Simulation tools were developed to facilitate system integration of DML. The driving point impedance for an infinite plate is used and radiation loading is neglected in the modeling. Although this may be sufficient for the present study, a more sophisticated modeling approach dealing with the frequency dependent mechanical impedance and the associated radiation loading of a flexible finite plate should be developed in the future to improve the accuracy of response prediction.

In order to compare the DML with the conventional speaker, an objective evaluation regarding frequency response, directional response, sensitivity, efficiency, and harmonic distortion was undertaken. Experimental results revealed that the DML suffered from an inherent problem of sensitivity and efficiency. To alleviate the problem, electronic compensation based on the H_2 model matching principle was developed. The experimental result demonstrated the improvement of overall performance by using the woofer and electronic compensation. Alongside with the other advantages of DML, the enhanced efficiency should improve its practicality in applications where high audio quality is demanded.

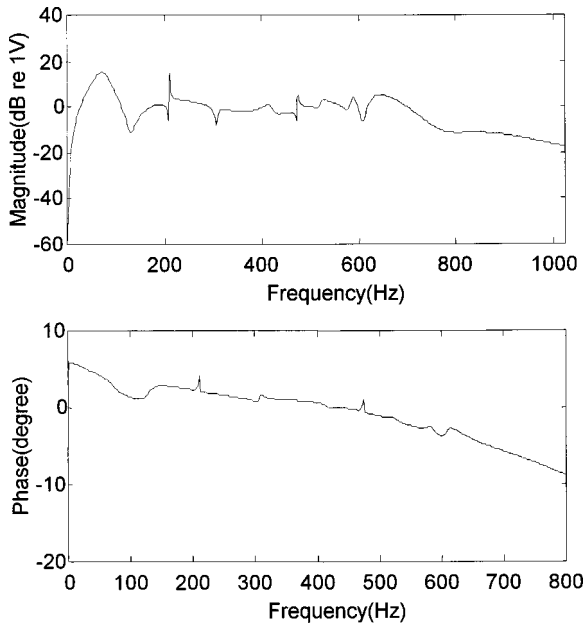

FIG. 17. Frequency response function of the H_2 feedforward controller.

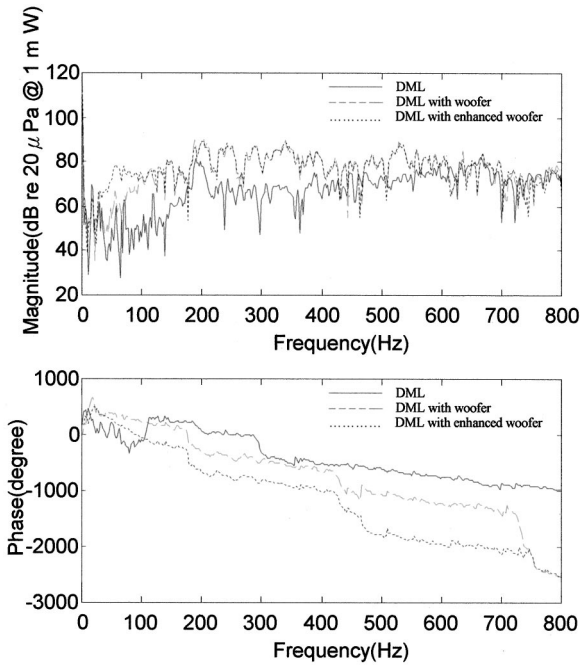

FIG. 18. Frequency response function of the DML system before and after enhancement: DML (solid line), DML with woofer (dash line), DML with enhanced woofer (dotted line). The measurements are under 1 m·W condition.

Although the compensated woofer proved to be a practical solution to the improvement of the overall efficiency, the bulky size of the woofer offsets somewhat the merits of DML. Furthermore, it should be noted that the efficiency problem of the DML alone has not been fundamentally changed in the present approach due to the physical constraint of flexible panels imposed by the sub-coincidence phenomenon. To further improve the efficiency of panel speakers, planar radiators without resort to the mechanism of flexural waves should be sought in the future. To summarize, the major limitations of the present work are: the use of impedance of infinite plate, the neglect of acoustic loading in circuit modeling, and the bass compensation by a conventional woofer. Research is currently on the way to circumvent these limitations.

ACKNOWLEDGMENTS

Special thanks are due to the illuminating discussions with New Transducers Limited, U.K. We also wish to thank Dr. William Thompson, Jr. of Applied Research Laboratory (ARL), Penn State University for lectures on acoustic transducers. The work was supported by the National Science Council (NSC) in Taiwan, Republic of China, under the Project No. NSC 89-2212-E009-057.

Azima, H. (**1998**). ''NXT Up against wall,'' *Audio Magazine*, September, pp. 34–41.
Beranek, L. L. (**1996**). *Acoustics* (Acoustical Society of America, Woodbury, NY).
Borwick, J. (**1994**). *Loudspeaker and Headphone Handbook* (Focal Press, Oxford, U.K.)
Cremer, L., and Heckl, M. (**1988**). *Structure-borne Sound* (Springer-Verlag, Berlin).
Doyle, J. C., Francis, B. A., and Tannenbaum, A. R. (**1992**). *Feedback Control Theory* (Macmillan, New York).
Grace, A., and Laub, A. J. (**1992**). MATLAB *Control System Toolbox* (Math Works, Natick, MA).
Harris, N., and Hawksford, M. O. (**1997**). ''The Distributed-Mode Loudspeaker (DML) as a Broadband Acoustic Radiator,'' The 103rd Convention of Audio Engineering Society Preprint, New York, September 1997, No. 4526 (D6).
ISO standard (**1977**). ''Basic Array of Microphone Positions in Free Field over a Reflecting Plane,'' ISO-3745-1977 (E).
Junger, M. C., and Feit, D. (**1986**). *Sound, Structures, and Their Interaction* (The MIT Press, Cambridge, MA).
Kinsler, L. E., Frey, A. R., Coppens, A. B., and Sanders, J. V. (**1982**). *Fundamentals of Acoustics* (Wiley, New York).
Leissa, A. (**1993**). *Vibration of Plates* (Acoustical Society of America, Woodbury, NY).
Morse, P. M., and Ingard, K. U. (**1986**). *Theoretical Acoustics* (Princeton University Press, Princeton, NJ).
Panzer, J. W., and Harris, N. (**1998a**). ''Distributed-Mode Loudspeaker Radiation Simulation,'' The 104th Convention of Audio Engineering Society Preprint, New York, No. 4783.
Panzer, J. W., and Harris, N. (**1998b**). ''Distributed Mode Loudspeaker Simulation Model,'' The 104th Convention of Audio Engineering Society Preprint, New York, No. 4739.